

# Voxel-Based Dosimetry Predicts Hepatotoxicity in Hepatocellular Carcinoma Patients Undergoing Radioembolization with $^{90}\text{Y}$ Glass Microspheres

Masao Watanabe<sup>1,2</sup>, Hong Grafe<sup>1,2</sup>, Jens Theysohn<sup>2,3</sup>, Benedikt Schaarschmidt<sup>2,3</sup>, Johannes Ludwig<sup>2,3</sup>, Leonie Jochheim<sup>2,4</sup>, Matthias Jeschke<sup>2,4</sup>, Hartmut Schmidt<sup>2,4</sup>, Wolfgang P. Fendler<sup>1,2</sup>, Alexandros Moraitis<sup>1,2</sup>, Ken Herrmann<sup>1,2</sup>, Kelsey L. Pomykala<sup>5</sup>, and Manuel Weber<sup>1,2</sup>

<sup>1</sup>Department of Nuclear Medicine, University Clinic Essen, Essen, Germany; <sup>2</sup>University of Duisburg–Essen and German Cancer Consortium–University Hospital, Essen, Germany; <sup>3</sup>Institute of Diagnostic and Interventional Radiology and Neuroradiology, University Clinic Essen, Essen, Germany; <sup>4</sup>Department of Gastroenterology and Hepatology, University Clinic Essen, Essen, Germany; and <sup>5</sup>Institute for AI in Medicine, University Medicine Essen, Essen, Germany

Personalized dosimetry holds promise to improve radioembolization treatment outcomes in hepatocellular carcinoma (HCC) patients. To this end, tolerance absorbed doses for nontumor liver tissue are assessed by calculating the mean absorbed dose to the whole nontumor liver tissue (AD-WNTLT), which may be limited by its neglect of nonuniform dose distribution. Thus, we analyzed whether voxel-based dosimetry could be more accurate in predicting hepatotoxicity in HCC patients undergoing radioembolization. **Methods:** In total, 176 HCC patients were available for this retrospective analysis; of these, 78 underwent partial- and 98 whole-liver treatment. Posttherapeutic changes in bilirubin were graded using the Common Terminology Criteria for Adverse Events. We performed voxel-based and multicompartment dosimetry using pretherapeutic  $^{99\text{m}}\text{Tc}$ -labeled human serum albumin SPECT and contrast-enhanced CT/MRI and defined the following dosimetry parameters: AD-WNTLT; the nontumor liver tissue volume exposed to at least 20 Gy (V20), at least 30 Gy (V30), and at least 40 Gy (V40); and the threshold absorbed dose to the 20% (AD-20) and 30% (AD-30) of nontumor liver tissue with the lowest absorbed dose. Their impact on hepatotoxicity after 6 mo was analyzed using the area under the receiver-operating-characteristic curve; thresholds were identified using the Youden index. **Results:** The area under the curve for prediction of posttherapeutic grade 3+ increases in bilirubin was acceptable for V20 (0.77), V30 (0.78), and V40 (0.79), whereas it was low for AD-WNTLT (0.67). The predictive value could further be increased in the subanalysis of patients with whole-liver treatment, where a good discriminatory power was found for V20 (0.80), V30 (0.82), V40 (0.84), AD-20 (0.80), and AD-30 (0.82) and an acceptable discriminatory power was found for AD-WNTLT (0.63). The accuracies of V20 ( $P = 0.03$ ), V30 ( $P = 0.009$ ), V40 ( $P = 0.004$ ), AD-20 ( $P = 0.04$ ), and AD-30 ( $P = 0.02$ ) were superior to that of AD-WNTLT but did not differ significantly from each other. The respective thresholds were 78% (V30), 72% (V40), and 43 Gy (AD-30). Statistical significance was not reached for partial-liver treatment. **Conclusion:** Voxel-based dosimetry may more accurately predict hepatotoxicity than multicompartment dosimetry in HCC patients undergoing radioembolization, which could enable dose escalation or deescalation with the intent to optimize treatment response. Our results indicate that a V40 of 72% may be particularly useful in whole-liver treatment. However, further research is warranted to validate these results.

**Key Words:** SIRT; liver toxicity; voxel-based dosimetry; multicompartment dosimetry; radioembolization

**J Nucl Med 2023; 00:1–7**

DOI: 10.2967/jnumed.122.264996

**O**n the basis of an ever-growing body of evidence, radioembolization guidelines and expert consensus increasingly recommend the use of multicompartment dosimetry, that is, treatment activity calculations based on a separate pretherapeutic assessment of mean absorbed doses to the tumor and nontumor tissue (1–4). Following these recommendations with regard to  $^{90}\text{Y}$  glass microspheres, the mean absorbed dose to the whole nontumor liver tissue (AD-WNTLT) should be kept below 75 Gy to minimize the risk of hepatic decompensation, although different thresholds based on baseline bilirubin have been proposed (4,5). However, when AD-WNTLT is used, nonuniform dose distribution is not considered. This could potentially be addressed by use of voxel-based dosimetry.

Three-dimensional voxel-based dosimetry evaluates the absorbed dose to each reconstructed voxel, thus taking into account dose heterogeneity and gradients in each region on a small spatial scale (3,6), which resembles absorbed dose planning models used in external-beam radiotherapy (7). However, the benefits of voxel-based activity calculation for  $^{90}\text{Y}$  radioembolization in hepatocellular carcinoma (HCC) have not yet been established (4). The limited spatial resolution of  $^{99\text{m}}\text{Tc}$ -macroaggregated albumin (MAA) SPECT used for pretherapeutic assessment of dose distribution in  $^{90}\text{Y}$  radioembolization may not be sufficient to map the voxel-based distribution of tumor lesions because of the presence of image noise and partial-volume effects (6). However, the volume of the nontumoral liver is typically larger by an order of magnitude than lesions, potentially allowing for voxel-based dosimetry of the nontumoral liver (8). In addition,  $^{99\text{m}}\text{Tc}$ -MAA SPECT predicts glass  $^{90}\text{Y}$  microsphere distribution more reliably in the nontumoral liver than in tumor lesions (3,8–10).

So far, there is no consensus on how to parametrize voxel-based dosimetry in radioembolization; however, exploratory considerations are facilitated by literature on external-beam radiation therapy and surgery. In external-beam radiation therapy, the safety threshold of the absorbed dose to the nontumor hepatic tissue ranges from 20 to 40 Gy

Received Oct. 5, 2022; revision accepted Mar. 7, 2023.

For correspondence or reprints, contact Manuel Weber (manuel.weber@uk-essen.de).

Published online Jun. 8, 2023.

COPYRIGHT © 2023 by the Society of Nuclear Medicine and Molecular Imaging.

(7,11,12), whereas in liver surgery, a remnant nontumor liver of 20% and 30% should be aimed for (13–17).

This work retrospectively investigated the prognostic impact of various voxel-based dosimetry parameters on short-term (6 mo) hepatotoxicity, compared with multicompartment dosimetry in HCC patients undergoing radioembolization with  $^{90}\text{Y}$  glass microspheres.

## MATERIALS AND METHODS

### Patients

From March 2008 to February 2021, 406 consecutive patients with HCC were screened from the radioembolization registry from our institution, and 176 were excluded because the follow-up period of their laboratory data was less than 6 mo. Of the remaining 230 patients, 3 underwent 2 radioembolization sessions to the identical target volume within 6 mo, impairing the assessment of absorbed dose distribution. Three patients underwent concurrent transarterial chemoembolization. Twenty-three patients underwent subsequent transarterial chemoembolization or radioembolization within 6 mo after the first radioembolization. In 25 patients, dosimetry calculations were not possible because of missing CT or MR images or technical issues. After exclusion of these 54 patients, 176 were finally included in this retrospective study (Fig. 1).

Of these 176 patients, 142 were male and 34 were female; the mean patient age was 67.2 y (range, 20 to 86 y). Seventy-eight patients underwent partial-liver treatment, and 98 underwent whole-liver treatment. Of the latter, 9 received a lobar injection after hemihepatectomy, making it a whole-liver treatment.

In cases of whole-liver treatment with 2 or more injections (e.g., separate injections for left and right lobes), injections were performed in 2 sessions, approximately 4–6 wk apart. The patient characteristics are summarized in Table 1. Of note, 3 patients had very limited extrahepatic metastases (adrenal gland,  $n = 1$ ; lung,  $n = 1$ , abdominal wall,  $n = 1$ ) (3). Seven patients had previously been treated with sorafenib and 1 patient with lenvatinib. In addition, 23 and 30 patients underwent transarterial chemoembolization or radiofrequency ablation and liver resection before radioembolization, respectively. Concerning this retrospective study, all procedures performed were approved in accordance with the ethical standards of the institutional review board of the Medical Faculty of the University Duisburg–Essen (Ethics Committee approval 13-5325BO) and with the principles of the Declaration of Helsinki and its later amendments. All patients gave written informed consent to the analysis of available data.

### Treatment Algorithm

All radioembolization cases were discussed by a multidisciplinary tumor board. Digital-subtraction angiography,  $^{99\text{m}}\text{Tc}$ -human serum albumin (HSA) planar scintigraphy, and SPECT/CT were performed for treatment planning. A mean of 151.4 MBq (range, 90–193 MBq) of  $^{99\text{m}}\text{Tc}$ -HSA was administered into the hepatic target vessels, and image acquisition started within 2 h. Images were acquired on a Symbia T2 (Siemens Medical Solutions AG) hybrid SPECT/CT scanner using a 130- to 150-keV energy window, and a total of 64 views were acquired in step-and-shoot mode, with 15 s per view and a 2.8° angular step size. The low-dose CT was performed immediately after emission acquisition. Images were reconstructed into a 128 × 128 matrix with a cubic voxel size of 4.8 mm<sup>3</sup> using the 3-dimensional ordered-subset expectation maximization algorithm with 8 iterations and 4 subsets and no smoothing filter. All images were corrected for scatter and attenuation.

Calculation of the lung-shunt fraction was based on the planar scintigraphy following guideline recommendations, and visceral shunting was assessed using  $^{99\text{m}}\text{Tc}$ -HSA SPECT/CT by 2 nuclear medicine physicians as per clinical routine. Treatment activity was calculated using unicompartiment dosimetry (mean perfused target volume absorbed dose, 80–150 Gy), aiming for an absorbed dose of 120 Gy ( $\pm 10\%$ ) to the perfused target volume, with further adjustments being based on factors such as liver function, tumor load,  $^{99\text{m}}\text{Tc}$ -HSA uptake, and the extent of the treated liver fraction. Treatment activity was injected while patient breathed freely in the same catheter position as for the pretherapeutic  $^{99\text{m}}\text{Tc}$ -HSA scan. The mean duration from dose calibration to the first and second dose injections was 4.5 d (range, 1–12 d).

### Dosimetry Calculation

Post hoc multicompartment and voxel-based dosimetry were performed by a board-certified nuclear medicine physician and radiologist in collaboration with a board-certified nuclear medicine physician using Mirada Simplicit90Y (Mirada Medical). The mean durations between the first radioembolization and the  $^{99\text{m}}\text{Tc}$ -HSA SPECT and between the  $^{99\text{m}}\text{Tc}$ -HSA SPECT and contrast-enhanced CT/MRI were 40.9 and 19.6 d, respectively.

After manual coregistration of contrast-enhanced CT/MR and  $^{99\text{m}}\text{Tc}$ -HSA SPECT/CT images, segmentation of whole-liver volume, perfused target volumes, tumor tissue, and nontumor liver tissue was performed both manually and automatically or semiautomatically by use of region-growing and thresholding tools. The whole-liver volume segmentation was performed automatically, whereas tumor lesions were segmented on CT/MR images using region-growing tools and on  $^{99\text{m}}\text{Tc}$ -HSA SPECT images using visually determined thresholds.

As for dosimetry calculation, we calculated the AD-WNTLT (multicompartment dosimetry) and determined the volume of nontumor liver tissue (voxel-based dosimetry), in which the absorbed doses exceeded 20 Gy (V20), 30 Gy (V30), and 40 Gy (V40). In addition, we determined the absorbed dose threshold level (voxel-based dosimetry) including a volume of 20% (AD-20) and 30% (AD-30) of the total nontumor liver tissue receiving the lowest absorbed doses; that is, 20% of the nontumor liver tissue received less than AD-20 and 30% of the nontumor liver tissue received less than AD-30. The analyses were limited to AD-20, AD-30, V20, V30, and V40 to prevent spurious results and multiple testing problems. The hepatic reserve, that is, the fraction of liver tissue not treated by radioembolization, was measured for all patients undergoing partial-liver treatment, and the percentage of hepatic tumor

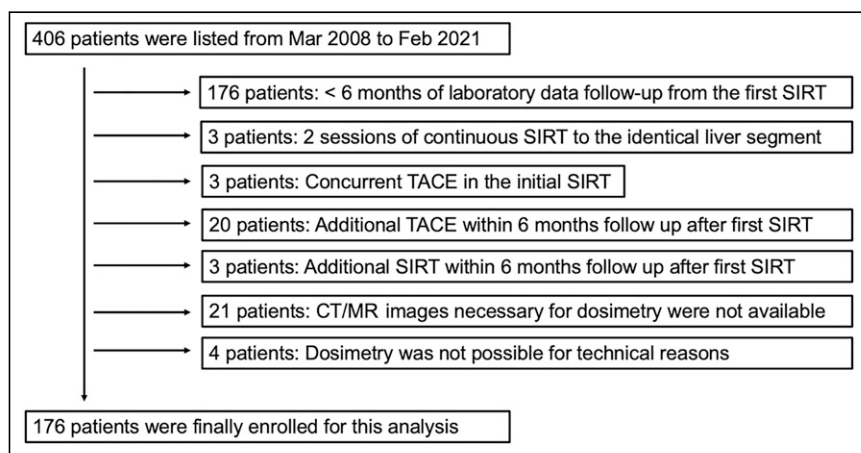


**FIGURE 1.** CONSORT (consolidated standard of reporting trial) diagram demonstrating patient enrollment. SIRT = selective internal radiation therapy; TACE = transarterial chemoembolization.

**TABLE 1**  
Patient Characteristics (*n* = 176)

Characteristic	Value	Characteristic	Value
Age (y)	67.2 ± 10.1 (range, 20–86)	ECOG score	
Sex		0	127
Male	142	1+	46
Female	34	NA	3
Origin of cirrhosis		Liver cirrhosis	
Alcohol	24	Positive	115
NASH	18	Negative	61
Hepatitis B	10	Tumor involvement	
Hepatitis C	22	<25%	147
Mixed or unknown	41	≥25%	29
Baseline AST (IU/L)	61.2 ± 47.0	SIRT procedure	
Baseline ALT (IU/L)	51.4 ± 45.8	Partial-liver	78
Baseline bilirubin (mg/dL)	0.8 ± 0.4	Whole-liver	98
Baseline albumin (g/dL)	4.2 ± 0.4	PV thrombosis (//)	
Child–Pugh score		Vp1–3	46
A	109	Vp4	9
B7	6	Negative	121
ALBI score		Tumor invasiveness (positive/negative)	
G1	53	Positive	86
G2	122	Negative	90
G3	1	Treatment-native patients before SIRT	125
BCLC score		Prior therapy*	
A	41	Liver resection	30
B	79	TACE or RFA	23
C	56	Sorafenib or lenvatinib	8

\*10/51 patients underwent several prior therapies.

NASH = nonalcoholic steatohepatitis; AST = aspartate transaminase; ALT = alanine transaminase; ALBI = albumin-bilirubin; BCLC = Barcelona Clinic liver cancer; ECOG = Eastern Cooperative Oncology Group; NA = not applicable; SIRT = selective internal radiation therapy; PV = portal vein; tumor invasiveness = tumor with irregular margins invading into surrounding tissues including nontumor liver tissue, portal vein, or hepatic vein; TACE = transarterial chemoembolization; RFA = radiofrequency ablation.

Qualitative data are number and percentage; continuous data are mean ± SD.

burden was obtained by dividing the tumor volume by the whole-liver volume as measured on contrast-enhanced CT/MRI.

#### Follow-up

The patients who underwent radioembolization were followed up using total bilirubin measurements for at least 6 mo (*n* = 176). Adverse effects were graded using the Common Terminology Criteria for Adverse Events (CTCAE), version 5. Relevant hepatotoxicity was defined as a binary metric by the occurrence of grade 3+ toxicity in bilirubin levels, on the basis of prior publications identifying it as a particularly suitable marker for hepatotoxicity after radioembolization (18,19).

#### Statistical Analysis

Statistics were analyzed using MedCalc, version 20.113-32 bit (MedCalc Software). To investigate the relationship between the absorbed dose of the nontumor liver and the liver toxicity within the follow-up period of 6 mo, we performed a receiver-operating-characteristic (ROC) curve analysis and identified the cutoffs using the Youden index. ROC curve analyses were compared using Hanley and McNeil's methodology (20). Subanalyses were performed for patients undergoing partial-liver

and whole-liver treatment; analyses of the latter group involved 9 patients undergoing lobar treatment after contralateral hemihepatectomy. A *P* value of less than 0.05 was considered statistically significant.

#### RESULTS

The mean volume and percentage of hepatic tumor burden across all patients were 269.0 mL (range, 0.6–2,534.4 mL) and 12.1% (range, 0.04%–61.1%), respectively. Twenty-nine patients had a high tumor burden (≥25%), and 147 patients had a low tumor burden (<25%). Of the 55 patients with portal tumoral thrombosis, 46 had the first branch or a more distal branch of the portal vein involved, and in 9 patients the main trunk of the portal vein was involved.

In the total cohort (*n* = 176), CTCAE grade 3+ hyperbilirubinemia was observed in 20 patients. Mean V20, V30, V40, AD-20, AD-30, and AD-WNTLT was 60.5%, 55.6%, 51.1%, 11.1 Gy, 18.2 Gy, and 57.7 Gy, respectively. Comparison of ROC curves (Fig. 2) showed superiority of V20 (area under the ROC curve [AUC], 0.77; *P* = 0.03), V30 (AUC, 0.78; *P* = 0.009), and V40

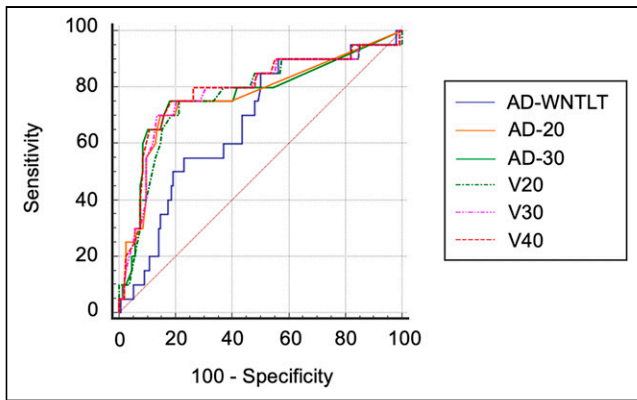


**FIGURE 2.** ROC analyses of whole patient cohort assessing relationship of absorbed dose parameters and occurrence of liver decompensation within 6 mo.

(AUC, 0.79;  $P = 0.005$ ) over AD-WNTLT (AUC, 0.67) in predicting 6-mo hepatotoxicity. V40 was significantly more accurate than V20 ( $P < 0.05$ ), whereas no difference was found between V40 and V30 ( $P = 0.09$ ). The cutoffs using the Youden index with the follow-up period of 6 mo, in consideration of the ROC analyses in CTCAE grade 3+ hyperbilirubinemia (Table 2; Figs. 2 and 3), were 56.9 Gy, 80%, 78%, 68%, 27 Gy, and 37 Gy in AD-WNTLT, V20, V30, V40, AD-20, and AD-30, respectively.

In the cohort that underwent partial-liver treatment ( $n = 78$ ), CTCAE grade 3+ hyperbilirubinemia was observed in 4 patients. Mean V20, V30, V40, AD-20, AD-30, AD-WNTLT, and hepatic reserve were 42.7%, 39.7%, 36.9%, 0.1 Gy, 1.4 Gy, 42.1 Gy, and 41.8%, respectively. The AUC of the voxel-based calculations ranged from 0.52 to 0.59 for voxel-based analyses and was 0.58 for AD-WNTLT; however, statistical significance was reached only for AD-30 ( $P < 0.001$ ). The cutoffs using the Youden index with the follow-up period of 6 mo, in consideration of the ROC analyses in CTCAE grade 3+ hyperbilirubinemia (Table 3; Fig. 4; Supplemental Fig. 1; supplemental materials are available at <http://jnm.snmjournals.org>), were 58.7 Gy, 6%, 6%, 5%, 0 Gy, 0 Gy, and 34% in AD-WNTLT, V20, V30, V40, AD-20, AD-30, and hepatic reserve, respectively.

In the cohort that underwent whole-liver treatment ( $n = 98$ ), CTCAE grade 3+ hyperbilirubinemia was observed in 16 of 98 within 6 mo and in 2 of 49 within 6–12 mo. Mean V20, V30, V40, AD-20, AD-30, and AD-WNTLT were 74.6%, 68.3%, 62.3%, 19.9 Gy, 31.6 Gy, and 70.2 Gy, respectively. The AUC of the

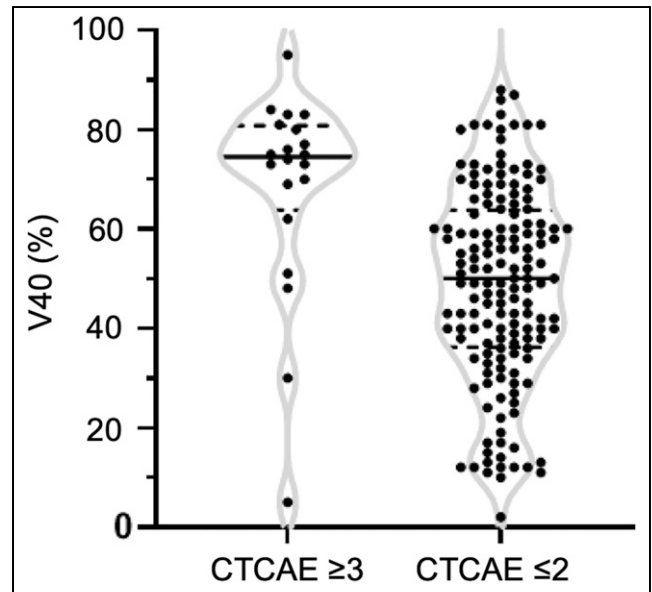


**FIGURE 3.** Scatterplot of whole patient cohort: comparison of V40 between group of CTCAE for hyperbilirubinemia adverse effects  $\geq 3$  and group of CTCAE  $\leq 2$ .

voxel-based calculations using histograms (V20, V30, V40, AD-20, and AD-30) (AUC, 0.80–0.84) were superior to that of the AD-WNTLT (AUC, 0.63) (Table 4; Figs. 5 and 6). V20 ( $P = 0.03$ ), V30 ( $P = 0.009$ ), V40 ( $P = 0.004$ ), AD-20 ( $P = 0.04$ ), and AD-30 ( $P = 0.02$ ) were superior to AD-WNTLT in predicting hepatotoxicity, whereas the predictive power between them did not differ significantly. The cutoffs were determined to be 55.6 Gy, 80%, 78%, 72%, 27 Gy, and 43 Gy in AD-WNTLT, V20, V30, V40, AD-20, and AD-30, respectively.

## DISCUSSION

Our results indicate superiority for voxel-based dosimetry in the pretherapeutic prediction of hepatotoxicity in HCC patients undergoing radioembolization of the whole liver. All tested voxel-based parameters were more accurate in predicting 6-mo hepatotoxicity than AD-WNTLT, which is considered the state of the art by current guidelines (3,4). A V40 of more than 72%, in particular, appears to be an accurate predictor of liver decompensation, showing an accuracy superior to V20, AD-20, AD-30, and AD-WNTLT and a tendency toward higher accuracy than V30.

**TABLE 2**  
ROC Analysis of 6-Month Toxicity of Whole Patient Cohort with 6-Month Follow-up (CTCAE Grade 3+ Hyperbilirubinemia, 20 Positive and 156 Negative)

Parameter	AD-WNTLT	V20	V30	V40	AD-20	AD-30
AUC	0.672	0.768	0.782	0.790	0.765	0.770
<i>P</i> value	0.006	<0.001	<0.001	<0.001	<0.001	<0.001
<i>P</i> value vs AD-WNTLT*		0.025	0.0094	0.0046	0.096	0.055
Cutoff	56.9 Gy	80%	78%	68%	27 Gy	37 Gy

\**P* value of ROC comparison between each voxel-based parameter and AD-WNTLT (multicompartment parameter); cutoff was determined by Youden index.

**TABLE 3**  
ROC Subanalysis of 6-Month Toxicity for Patients Who Underwent Partial Liver Treatment (CTCAE Grade 3+ Hyperbilirubinemia, 4 Positive and 74 Negative)

Parameter	AD-WNTLT	HR	V20	V30	V40	AD-20	AD-30
AUC	0.578	0.591	0.534	0.546	0.542	0.520	0.588
P value	0.629	0.452	0.868	0.811	0.818	0.079	<0.001
P value vs AD-WNTLT*		0.90	0.41	0.45	0.30	0.72	0.95
Cutoff	58.7 Gy	33.8%	6%	6%	5%	0 Gy	0 Gy

\*P value of ROC comparison between each voxel-based parameter and AD-WNTLT (multicompartment parameter); cutoff was determined by Youden index.

HR = hepatic reserve, that is, liver volume not treated by radioembolization.

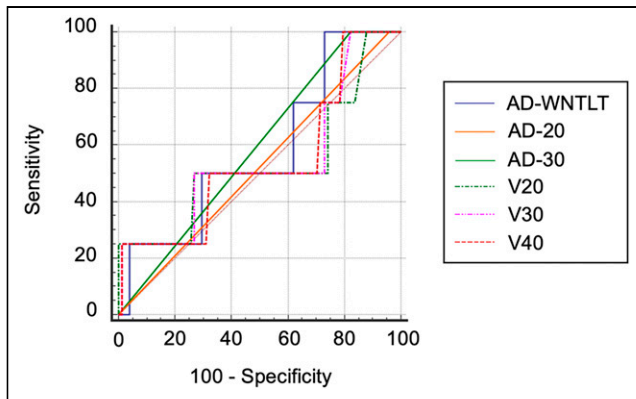


**FIGURE 4.** ROC analyses of patients undergoing partial-liver radioembolization assessing relationship of absorbed dose parameters and occurrence of liver decompensation within 6 mo.

Of all patients undergoing whole-liver treatment, grade 3+ hepatotoxicity was observed in only 3 of 98 patients with a V40 of no more than 72%, making it a reasonably safe threshold for radioembolization. On the basis of these results, activity escalation within safe margins would have been possible in 65 of 98 patients with a V40 of less than 72% undergoing whole-liver radioembolization. Because prior studies assessing the absorbed dose–response relationship for HCC lesions treated with radioembolization show a wide range of proposed absorbed dose thresholds, it follows that additional increases in tumor-absorbed doses may further increase the likelihood of treatment response (19,21,22).

Treatment planning using absorbed dose to the nontumor liver tissue as an additional driving criterion may be of particular interest in the presence of small tumor lesions, where partial-volume effects are expected to lead to a severe underestimation of absorbed doses. Furthermore, the prediction of absorbed doses to nontumor liver tissue by use of  $^{99m}\text{Tc}$ -MAA has been shown to be more reliable than the prediction of absorbed doses to tumor lesions, underpinning the robustness of this approach (9,10).

To our knowledge, this is the first study to show superiority for voxel-based dosimetry over multicompartment dosimetry in the prediction of liver decompensation of HCC patients undergoing radioembolization with  $^{90}\text{Y}$  glass microspheres. However, prior studies have shown some evidence for a potential benefit of voxel-based dosimetry to assess the likelihood of treatment response. Two retrospective studies of patients with liver tumors showed that voxel-based dosimetry of tumor lesions as assessed on posttherapeutic PET was predictive of tumor response after radioembolization with  $^{90}\text{Y}$  resin microspheres (23,24). Similarly, a slightly higher accuracy than for multicompartment dosimetry was found for response prediction using voxel-based segmentation of the pretherapeutic  $^{99m}\text{Tc}$ -MAA SPECT/CT images (25).

The analysis of prognostic parameters of hepatotoxicity in HCC patients undergoing partial-liver treatment did not reveal statistically significant results. This may be attributable to low statistical power because of a low event rate in this subcohort. In addition, the prognostic impact of the voxel-based parameters chosen for this study may not be able to accurately reflect radiobiologic effects in a patient cohort, in whom a relevant part of the liver remains untreated.

**TABLE 4**  
ROC Subanalysis of 6-Month Toxicity for Patients Who Underwent Whole Liver Treatment (CTCAE Grade 3+ Hyperbilirubinemia, 16 Positive and 82 Negative)

Parameter	AD-WNTLT	V20	V30	V40	AD-20	AD-30
AUC	0.633	0.796	0.824	0.840	0.803	0.823
P value	0.042	<0.001	<0.001	<0.001	<0.001	<0.001
P value vs AD-WNTLT*		0.032	0.0088	0.0038	0.041	0.015
Cutoff	55.6 Gy	80%	78%	72%	27 Gy	43 Gy

\*P value of ROC comparison between each voxel-based parameter and AD-WNTLT (multicompartment parameter); cutoff was determined by Youden index.

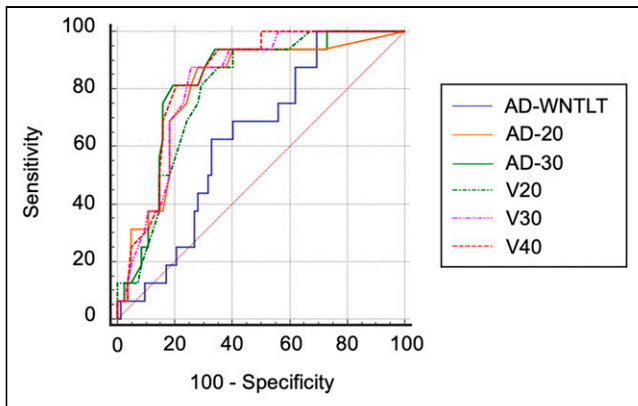


**FIGURE 5.** ROC analyses of patients undergoing whole-liver radioembolization assessing relationship of absorbed dose parameters and occurrence of liver decompensation within 6 mo.

Limitations of this study include the high rate of patients with insufficient follow-up, as well as its retrospective nature. In addition, absorbed dose distribution was derived from pretherapeutic  $^{99m}\text{Tc}$ -HSA SPECT/CT, which has been shown to be a reliable but not perfect predictor of  $^{90}\text{Y}$  glass microsphere deposition (9,10). Calculated doses will therefore deviate from those achieved during treatment, posing inherent constraints on the reliability of  $^{99m}\text{Tc}$ -MAA/HSA-based pretherapeutic prediction of liver decompensation. On the other hand,  $^{99m}\text{Tc}$ -MAA/HSA SPECT/CT constitutes the only modality to pretherapeutically assess  $^{90}\text{Y}$  microsphere deposition recommended by current guidelines, with no viable alternatives. In addition, for sequential bilobar radioembolization, absorbed doses from both sessions were analyzed cumulatively, with no interim  $^{99m}\text{Tc}$ -MAA/HSA SPECT/CT or contrast-enhanced CT, meaning that volumetric changes between treatments were not considered. Though technically a limitation with regard to accurate assessment of dose distribution, this more closely resembles the clinical reality of most physicians and is therefore preferable. The interval from the  $^{99m}\text{Tc}$ -MAA/HSA

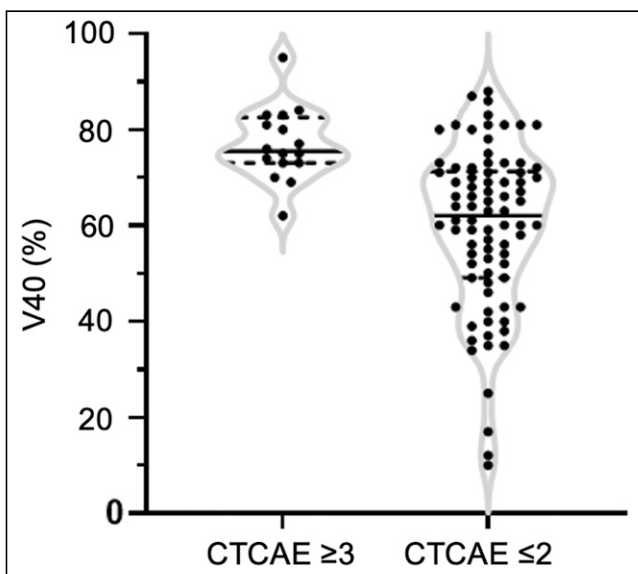


**FIGURE 6.** Scatterplot of whole-liver treatment patients: comparison of V40 between group of CTCAE for hyperbilirubinemia adverse effects  $\geq 3$  and group of CTCAE  $\leq 2$ .

SPECT/CT scan to the first radioembolization (40.9 d) was longer than ideal (15 d) (3) and may limit the reliability of the predicted dose distribution.

## CONCLUSION

Our retrospective study showed encouraging results for the prediction of posttherapeutic liver decompensation in HCC patients after whole-liver radioembolization with  $^{90}\text{Y}$  glass microspheres using voxel-based absorbed dose metrics. In these patients, exposure of 72% or more of the nontumor liver tissue to more than 40 Gy was associated with an increased risk of liver decompensation. Future research is warranted to confirm these preliminary results and elucidate the interplay of dosimetry results and baseline laboratory and clinical parameters.

## DISCLOSURE

Benedikt M. Schaarschmidt received a research grant from PharmaCept for an undergoing investigator-initiated study not related to this paper. Wolfgang P. Fendler is a consultant for Endocyte and BTG and received fees from RadioMedix, Bayer, and Parexel outside the submitted work. Wolfgang P. Fendler reports fees from SOFIE Bioscience (research funding), Janssen (consultant, speakers' bureau), Calyx (consultant), Bayer (consultant, speakers' bureau, research funding), Parexel (image review), and AAA (speakers' bureau) outside the submitted work. Ken Herrmann reports personal fees from Bayer, Sofie Biosciences, SIRTEX, Adacap, Curium, Endocyte, BTG, IPSEN, Siemens Healthineers, GE Healthcare, Amgen, Novartis, ymabs, Aktis Oncology, Theragnostics, and Pharma15; other fees from Sofie Biosciences; nonfinancial support from ABX; and grants from BTG outside the submitted work. Manuel Weber reports personal fees from Boston Scientific, Terumo, Advanced Accelerator Applications, and Eli Lilly outside the submitted work. No other potential conflict of interest relevant to this article was reported.

## KEY POINTS

**QUESTION:** Can voxel-based dosimetry predict hepatotoxicity in HCC patients undergoing radioembolization and thereby improve pretherapeutic activity calculation?

**PERTINENT FINDINGS:** Voxel-based dosimetry may more accurately predict hepatotoxicity than multicompartment dosimetry, which is currently considered to be the state of the art in procedure guidelines.

**IMPLICATIONS FOR PATIENT CARE:** Voxel-based dosimetry of selective internal radiation therapy is helpful to assess expected hepatotoxicity and may thereby enable safe escalation or deescalation of treatment activity to optimize tumor control, that is, the efficacy and toxicity trade-off of selective internal radiation therapy.

## REFERENCES

- Garin E, Tselikas L, Guiu B, et al. Personalised versus standard dosimetry approach of selective internal radiation therapy in patients with locally advanced hepatocellular carcinoma (DOSISPHERE-01): a randomised, multicentre, open-label phase 2 trial. *Lancet Gastroenterol Hepatol.* 2021;6:17–29.
- Levillain H, Bagni O, Deroose CM, et al. International recommendations for personalised selective internal radiation therapy of primary and metastatic liver diseases with yttrium-90 resin microspheres. *Eur J Nucl Med Mol Imaging.* 2021;48:1570–1584.

3. Weber M, Lam M, Chiesa C, et al. EANM procedure guideline for the treatment of liver cancer and liver metastases with intra-arterial radioactive compounds. *Eur J Nucl Med Mol Imaging*. 2022;49:1682–1699.
4. Salem R, Padia SA, Lam M, et al. Clinical and dosimetric considerations for Y90: recommendations from an international multidisciplinary working group. *Eur J Nucl Med Mol Imaging*. 2019;46:1695–1704.
5. Chiesa C, Mira M, Bhoori S, et al. Radioembolization of hepatocarcinoma with <sup>90</sup>Y glass microspheres: treatment optimization using the dose-toxicity relationship. *Eur J Nucl Med Mol Imaging*. 2020;47:3018–3032.
6. Chiesa C, Sjøgreen-Gleisner K, Walrand S, et al. EANM dosimetry committee series on standard operational procedures: a unified methodology for <sup>99m</sup>Tc-MAA pre- and <sup>90</sup>Y peri-therapy dosimetry in liver radioembolization with <sup>90</sup>Y microspheres. *EJNMMI Phys*. 2021;8:77.
7. Apisarnthanarax S, Barry A, Cao M, et al. External beam radiation therapy for primary liver cancers: an ASTRO clinical practice guideline. *Pract Radiat Oncol*. 2022;12:28–51.
8. Haste P, Tann M, Persohn S, et al. Correlation of technetium-99m macroaggregated albumin and yttrium-90 glass microsphere biodistribution in hepatocellular carcinoma: a retrospective review of pretreatment single photon emission CT and posttreatment positron emission tomography/CT. *J Vasc Interv Radiol*. 2017;28:722–730.e1.
9. Gnesin S, Canetti L, Adib S, et al. Partition model-based <sup>99m</sup>Tc-MAA SPECT/CT predictive dosimetry compared with <sup>90</sup>Y TOF PET/CT posttreatment dosimetry in radioembolization of hepatocellular carcinoma: a quantitative agreement comparison. *J Nucl Med*. 2016;57:1672–1678.
10. Jadoul A, Bernard C, Lovinfosse P, et al. Comparative dosimetry between <sup>99m</sup>Tc-MAA SPECT/CT and <sup>90</sup>Y PET/CT in primary and metastatic liver tumors. *Eur J Nucl Med Mol Imaging*. 2020;47:828–837.
11. Burman C, Kutcher GJ, Emami B, Goitein M. Fitting of normal tissue tolerance data to an analytic function. *Int J Radiat Oncol Biol Phys*. 1991;21:123–135.
12. Emami B, Lyman J, Brown A, et al. Tolerance of normal tissue to therapeutic irradiation. *Int J Radiat Oncol Biol Phys*. 1991;21:109–122.
13. TheraSphere<sup>®</sup> yttrium-90 glass microspheres. Package insert. Biocompatibles UK Ltd.; revision 12.
14. Guglielmi A, Ruzzenente A, Conci S, Valdegamberi A, Iacono C. How much remnant is enough in liver resection? *Dig Surg*. 2012;29:6–17.
15. Kim HJ, Kim CY, Hur YH, et al. Comparison of remnant to total functional liver volume ratio and remnant to standard liver volume ratio as a predictor of postoperative liver function after liver resection. *Korean J Hepatobiliary Pancreat Surg*. 2013;17:143–151.
16. Garin E, Lenoir L, Edeline J, et al. Boosted selective internal radiation therapy with <sup>90</sup>Y-loaded glass microspheres (B-SIRT) for hepatocellular carcinoma patients: a new personalized promising concept. *Eur J Nucl Med Mol Imaging*. 2013;40:1057–1068.
17. Garin E, Rolland Y, Pracht M, et al. High impact of macroaggregated albumin-based tumour dose on response and overall survival in hepatocellular carcinoma patients treated with <sup>90</sup>Y-loaded glass microsphere radioembolization. *Liver Int*. 2017;37:101–110.
18. Braat MN, van Erpecum KJ, Zonnenberg BA, van den Bosch MA, Lam MG. Radioembolization-induced liver disease: a systematic review. *Eur J Gastroenterol Hepatol*. 2017;29:144–152.
19. Lam M, Garin E, Maccauro M, et al. A global evaluation of advanced dosimetry in transarterial radioembolization of hepatocellular carcinoma with yttrium-90: the TARGET study. *Eur J Nucl Med Mol Imaging*. 2022;49:3340–3352.
20. Hanley JA, McNeil BJ. A method of comparing the areas under receiver operating characteristic curves derived from the same cases. *Radiology*. 1983;148:839–843.
21. Kappadath SC, Mikell J, Balagopal A, Baladandayuthapani V, Kaseb A, Mahvash A. Hepatocellular carcinoma tumor dose response after <sup>90</sup>Y-radioembolization with glass microspheres using <sup>90</sup>Y-SPECT/CT-based voxel dosimetry. *Int J Radiat Oncol Biol Phys*. 2018;102:451–461.
22. Roosen J, Klaassen NJM, Westlund Gotby LEL, et al. To 1000 Gy and back again: a systematic review on dose-response evaluation in selective internal radiation therapy for primary and secondary liver cancer. *Eur J Nucl Med Mol Imaging*. 2021;48:3776–3790.
23. Kao YH, Steinberg JD, Tay YS, et al. Post-radioembolization yttrium-90 PET/CT—part 2: dose-response and tumor predictive dosimetry for resin microspheres. *EJNMMI Res*. 2013;3:57.
24. Allimant C, Kafrouni M, Delicque J, et al. Tumor targeting and three-dimensional voxel-based dosimetry to predict tumor response, toxicity, and survival after yttrium-90 resin microsphere radioembolization in hepatocellular carcinoma. *J Vasc Interv Radiol*. 2018;29:1662–1670 e1664.
25. Chiesa C, Bardies M, Zaidi H. Voxel-based dosimetry is superior to mean absorbed dose approach for establishing dose-effect relationship in targeted radionuclide therapy. *Med Phys*. 2019;46:5403–5406.